

Low-temperature X-ray structural studies of the ester and ether derivatives of *cis*- and *trans*-4-*tert*-butyl cyclohexanol and 2-adamantanol: application of the *variable oxygen probe* to determine the relative σ -donor ability of C–H and C–C bonds

Marisa Spiniello and Jonathan M. White*

School of Chemistry, The University of Melbourne, Victoria, 3010, Australia.

E-mail: whitejm@unimelb.edu.au

Received 31st March 2003, Accepted 26th June 2003

First published as an Advance Article on the web 28th July 2003

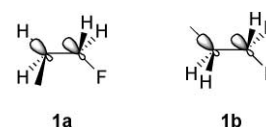
Results of low-temperature X-ray structural studies for five *cis*-, and three *trans*-4-*tert*-butyl cyclohexanol, and six 2-adamantanol ester and ether derivatives are reported. Plots of C–OR bond distance against $pK_a(\text{ROH})$ for derivatives of axial alcohol (**5**), equatorial alcohol (**6**) and 2-adamantanol derivatives (**7**) give slopes of -2.77×10^{-3} , -2.86×10^{-3} and -3.05×10^{-3} , respectively. Given that the relative differences in the slopes are modest, no clear distinction can be made about the relative σ -donor ability of a C–H bond and a C–C bond.

Introduction

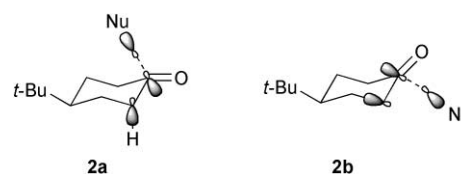
Baker and Nathan¹ reported that reaction of *p*-alkyl-substituted benzyl bromides with a solution of pyridine in acetone follows the reactivity order of; Me > Et > Prⁱ > Bu^t. This same order of reactivity was observed for many other reactions which were believed to involve electron deficient centres either directly on, or immediately adjacent to the aromatic ring. Baker and Nathan attributed this order of reactivity to C–H hyperconjugation, which was proposed to be superior to C–C hyperconjugation. This was supported by Taft and Lewis² who separated the contributions of inductive effects and resonance effects for several alkyl substituents for reactions ranging from the ionisation of alkyl-substituted benzoic acid derivatives, to the solvolysis rates of benzyl hydriyl chlorides (Ar(C₆H₅)CHCl), and came to the conclusion that C–H hyperconjugation is about 1.3 times more effective than C–C hyperconjugation.

Nevertheless both the origin of the Baker–Nathan effect and the relative merits of C–H and C–C hyperconjugation is still subject to much controversy. It has been suggested that the original Baker–Nathan effect is a solvation phenomenon and does not necessarily reflect differing merits of C–H and C–C hyperconjugation. For example Glyde and Taylor³ measured the pyrolysis rates of alkyl-substituted 1-aryl ethyl esters. This reaction has been shown to proceed *via* formation of a partial carbocation at the side-chain α -carbon,⁴ and therefore provided an ideal system to investigate the electron-releasing effects of alkyl substituents in the gas phase. They found the *tert*-butyl group to be significantly more electron releasing than the methyl group ($\sigma^+(\text{Bu}^t)/\sigma^+(\text{Me}) = 1.26$), and furthermore $\sigma_p^+ - \sigma_I$ for *t*-butyl (0.291) is greater than $\sigma_p^+ - \sigma_I$ for methyl (0.244). The data suggested that indeed the Baker–Nathan order of electron release by alkyl groups was a solvation phenomenon, and also that C–C hyperconjugation is greater than C–H hyperconjugation. However, Happer and Cooney⁵ determined the electronic effect of alkyl substituents by measuring their influence on the ¹³C NMR chemical shifts of the β -carbon of β -substituted styrenes. They found that the order of electron release by *p*-alkyl substituents was Me > Et > Prⁱ > Bu^t, which is the original Baker–Nathan order. Furthermore they found that this order was maintained in solvents ranging from CCl₄, CDCl₃ to Me₂SO and EtOH and concluded that the Baker–Nathan order can justifiably be attributed to superior C–H hyperconjugation. Rablen and co-workers⁶ reported a theoretical investigation on the *gauche* effect in 1-fluoropropane and

other 2-substituted-1-fluoroethanes. They concluded that the *gauche* conformation of 1-fluoropropane **1a** was preferred because it maximises overlap between the C–H σ -donor and the C–F σ^* acceptor orbital. The anti conformation **1b**, although sterically more favourable, was proposed to be disfavoured because it has the weaker C–C donor orbital interacting with the C–F σ^* orbital. From their calculations they established the following ranking of hyperconjugative electron donor abilities: C–Si > C–H > C–C > C–F.



Despite the fact that the relative σ -donor abilities of C–H and C–C bonds is still a matter of some dispute, Cieplak⁷ hypothesises that the preferred axial approach (**2a**) of small nucleophiles to cyclohexanone derivatives arises because of superior C–H hyperconjugation of the axial hydrogens with the developing Nu–C antibonding orbital.

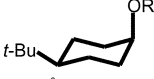



Given the conflicting data on the relative merits of C–H and C–C hyperconjugation, we were interested to establish whether useful information could be obtained from accurate X-ray structural studies of *cis* and *trans* ester derivatives of 4-*tert*-butyl cyclohexanol at low temperature.

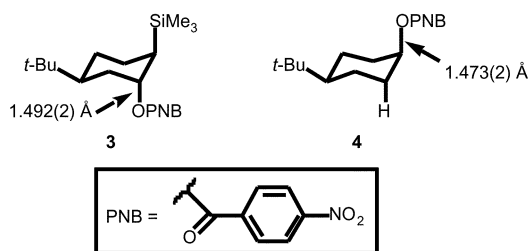
It has been demonstrated that C–O bond distances are sensitive to the effects of hyperconjugative electron donation into the C–O antibonding orbital.^{8–12} For example, the C–OPNB bond distances in the β -trimethylsilyl ester **3** is 1.492(2) Å,¹⁰ this is significantly lengthened with respect to the corresponding silicon-free analogue **4** which has a C–O distance of 1.473(2) Å.¹³ In **3** the C–Si bond, which is a strong σ -donor, overlaps and interacts with the C–OPNB σ^* orbital. Whereas in **4** the C–Si bond is replaced by a weaker C–H σ -donor orbital and as a result the C–OPNB bond is shorter.

In axial cyclohexanol derivatives **5** the C–O σ^* orbital overlaps with two antiperiplanar C–H bonds whereas in equatorial

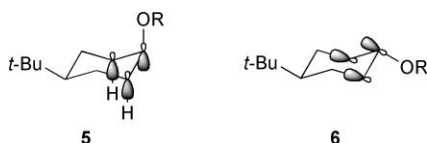
Table 1 C–O Bond distances in selected axial and equatorial cyclohexyl ester and ether derivatives

pK_a^a	R	 $r_{C-O}/\text{\AA}$	 $r_{C-O}/\text{\AA}$
3.43 ¹⁷	4-NO ₂ C ₆ H ₄ CO	5a 1.473(2)	6a 1.463(2)
			Molecule 1
			6a 1.468(2)
			Molecule 2
2.00 ¹⁸	2,4-(NO ₂) ₂ C ₆ H ₃ SO	5b 1.476(2)	6b 1.473(2)
0.42 ^{b,17}	2,4,6-(NO ₂) ₃ C ₆ H ₂	5c 1.497(2)	6c 1.491(2)
-3.80 ¹⁹	4-NO ₂ C ₆ H ₄ SO ₂	5d 1.492(2)	6d 1.487(2)

^a All pK_a values were measured in water at 25°C. ^b This pK_a value was measured at 24°C.



derivatives **6** the interaction is with the two antiperiplanar C–C bonds in the cyclohexane ring.



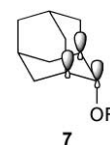
Do the differing σ -donor abilities of C–H and C–C bonds (if any) manifest in differences of the C–OR bond distances between the axial and equatorial derivatives? Although Kirby and co-workers⁹ found no evidence for this from room-temperature structural data, we were hopeful that the increased accuracy and precision of low-temperature X-ray data would allow us to determine any differences in axial and equatorial C–O bond distances (if indeed they exist).

We have previously reported, for different reasons, four pairs of axial and equatorial cyclohexanol derivatives; the *p*-nitrobenzoates **5a**¹³ and **6a**,¹³ the 2,4-dinitrobenzenesulfonates **5b**¹¹ and **6b**,¹⁴ the 2,4,6-trinitrophenoxides **5c**¹⁵ and **6c**,¹⁵ and the *p*-nitrobenzenesulfonates **5d**¹⁶ and **6d**¹⁶ (Table 1). In all four pairs of structures the axial C–OR bond distance is slightly longer than the equatorial distance. Although the differences within each pair of structures is small and barely significant in some cases, the fact that the same pattern is observed for all pairs strongly suggested to us that this difference is real.

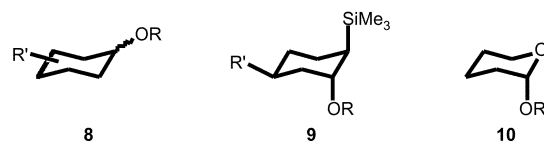
The slightly longer C–OR bond distances in the axial derivatives **5a–d** does not necessarily reflect the more effective σ -donor ability of the antiperiplanar C–H bonds in **5a–d**, compared with the antiperiplanar C–C bonds in **6a–d**, but may simply arise because axially disposed oxygen substituents are in a different steric environment to equatorial C–O substituents.

We decided to approach this question in two ways; firstly to determine the structures of ether and ester derivatives of 2-adamantanol **7**, in which the oxygen substituent is axial as in **5** but rather than having two C–H bonds antiperiplanar to the C–OR bond, there are two C–C bonds as in **6**.

The second approach was to apply the *variable oxygen probe*^{10,11} to determine any differences in the σ -donor abilities of C–H and C–C bonds. The *variable oxygen probe* is an X-ray



structural method for detecting the presence of electronic interactions between electron donors and oxygenated substituents in the ground state. Kirby and co-workers^{8,9} established that the C–O bond distance in the C–OR fragment increases with increasing electron demand of the OR substituent, reflecting an increasing contribution of the C⁺–OR valence bond form to the ground state structure. If the electron demand of a substituent OR is quantified as the pK_a value for the parent acid (ROH), then a plot of C–OR bond distance vs. pK_a (ROH) is linear, and the slope of the resulting plot is sensitive to the effects of electron donation into the C–OR σ^* antibonding orbital. The presence of good donor orbitals vicinal and antiperiplanar to the C–O bond results in a strong response of the C–OR distance to the electron demand of OR. This is because of increased stabilisation of the cation part of the valence bond form C⁺–OR. For example, the plots of C–OR bond distance vs. pK_a (ROH) constructed for **8**,⁹ **9**¹⁸ and **10**⁸ give the following relationships:



$$\mathbf{8}: r_{C-O}/\text{\AA} = 1.475 - 2.90 \times 10^{-3} pK_a(\text{ROH}); R^2 = 0.999 \quad (1)$$

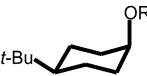

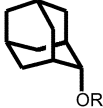
$$\mathbf{9}: r_{C-O}/\text{\AA} = 1.502 - 5.30 \times 10^{-3} pK_a(\text{ROH}); R^2 = 0.986 \quad (2)$$

$$\mathbf{10}: r_{C-O}/\text{\AA} = 1.493 - 6.49 \times 10^{-3} pK_a(\text{ROH}); R^2 = 0.985 \quad (3)$$

A strong response of C–OR bond distance to the electron demand of OR is demonstrated for **10** which has oxygen lone pair (n_o) orbital antiperiplanar to the OR substituent (this is the basis of the well known anomeric effect),⁸ a strong response is also observed for **9** which has a C–Si bond antiperiplanar to the OR substituent (this is the basis of the silicon β -effect),¹⁰ but a weaker response is obvious in **8** which has either a σ C–H or C–C bonding orbital, which are both weaker donor orbitals situated antiperiplanar to the OR bond.

In this study we proposed to construct plots of C–OR bond distance vs. pK_a (ROH) for a range of ester and ether derivatives of **5**, **6** and **7** in the hope the electronic interaction between the donor and acceptor orbitals, which is reflected in the slopes obtained, might give some information about the σ -donor abilities of C–H and C–C bonds.

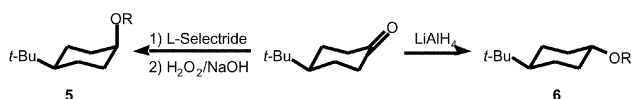
Table 2 Ester and ether derivatives of **5**, **6** and **7** suitable for low temperature X-ray analysis

pK_a^a		pK_a		pK_a	
7.15 ¹⁷	5e 4-NO ₂ C ₆ H ₄	2.17 ¹⁷	6e 2-NO ₂ C ₆ H ₄ CO	7.15 ¹⁷	7a 4-NO ₂ C ₆ H ₄
3.29 ²²	5f 3-NO ₂ -4-ClC ₆ H ₃ CO	-2.70 ¹⁹	6f 4-CH ₃ C ₆ H ₅ SO ₂	3.46 ¹⁷	7b 3-NO ₂ C ₆ H ₄ CO
2.85 ²³	5g 3,5-(NO ₂) ₂ C ₆ H ₃ CO	-2.80 ¹⁹	6g C ₆ H ₅ SO ₂	1.43 ¹⁷	7c 2,4-(NO ₂) ₂ C ₆ H ₃ CO
1.43 ²³	5h 2,4-(NO ₂) ₂ C ₆ H ₃ CO			-1.90 ¹⁹	7d CH ₃ SO ₂
0.66 ^{b 17}	5i Cl ₃ CCO			-2.70 ¹⁹	7e 4-CH ₃ C ₆ H ₅ SO ₂
				-2.80 ¹⁹	7f C ₆ H ₅ SO ₂

^a All pK_a values were measured in water at 25°C. ^b This pK_a value was measured at 20°C.

Results and discussion: synthesis

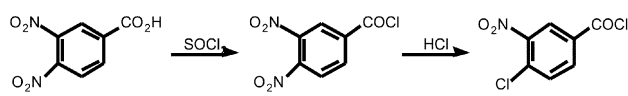
The alcohols **5** and **6** were prepared according to Scheme 1 by reduction with either lithium aluminium hydride²⁰ giving the equatorial alcohol **6** as the major product, or by reduction with L-selectride²¹ giving the axial alcohol **5**. 2-Adamantanol is commercially available.



Scheme 1

The alcohols **5**, **6** and **7** were converted to a wide range of ester and ether derivatives using standard techniques, those derivatives which gave crystals suitable for X-ray analysis and which could be cooled to low temperature without destructive phase changes are given in Table 2.

The chloronitrobenzoate **5f** was unexpectedly prepared from 3,4-dinitrobenzoic acid, which upon treatment with oxalyl chloride gave 3-nitro-4-chlorobenzoyl chloride by apparent displacement of the nitrite ion from 3,4-dinitrobenzoyl chloride, Scheme 2.



Scheme 2

Results and discussion: molecular structures

All structures were determined at 130 K to minimise the effects of thermal motion. Thermal ellipsoid plots for **5h**, **6e**, **7a** and **7c** are presented in Figs. 1, 2, 3 and 4, respectively (the remaining structures which have the same numbering system for the

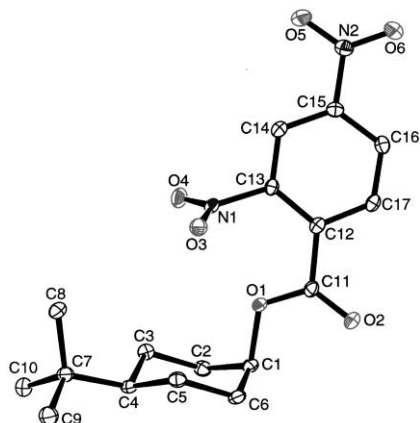


Fig. 1 ORTEP-3³⁶ representation of the molecular structure of **5h**. Thermal ellipsoids are drawn at the 30% probability level.

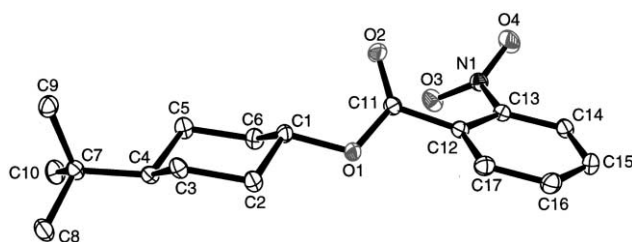


Fig. 2 ORTEP-3³⁶ representation of the molecular structure of **6e**. Thermal ellipsoids are drawn at the 30% probability level.

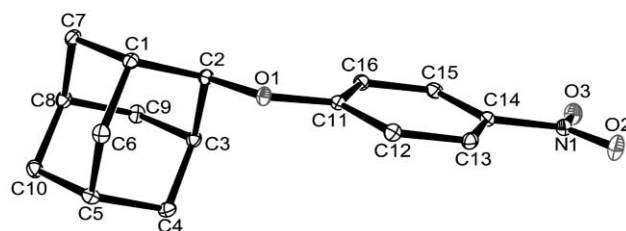


Fig. 3 ORTEP-3³⁶ representation of the molecular structure of **7a**. Thermal ellipsoids are drawn at the 30% probability level.

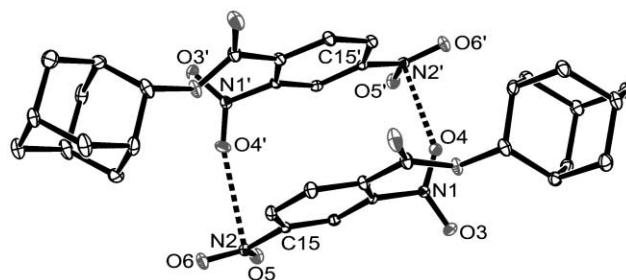


Fig. 4 ORTEP-3³⁶ representation of the molecular structure of **7c**, indicating the N...O distances (O(4)···N(2') = 2.789(2) Å; O(4')···N(2) = 2.851(2) Å) by dashed lines. Thermal ellipsoids are drawn at the 20% probability level.

cyclohexyl and adamantyl fragments are omitted for the purposes of brevity). Selected structural parameters for the axial derivatives **5a–5i**, the equatorial derivatives **6a–6g**, and the 2-adamantanyl derivatives **7a–7f** are presented in Tables 3, 4 and 5, respectively.

Structures **6g** and **7c** occur in the solid state with two independent molecules in the asymmetric unit. The two molecules of **6g** differ with respect to the conformation of the benzenesulfonate group; in one molecule the aromatic ring eclipses one of the S=O double bonds ($C_{ortho}-C_{ipso}-SO = 3.1(2)^\circ$) whereas in the second molecule the equivalent dihedral angle is $34.9(2)^\circ$. In **7c** the two independent molecules in the asymmetric unit are held together by a combination of π -stacking between the benzene rings, and nitro–nitro interactions (Fig. 4). The overall 'complex' has an approximate, non-crystallographic 2-fold axis of symmetry. The distance between the aromatic

Table 3 Selected bond distances (Å) for the axial derivatives **5a–5i**

Compound	C(1)–O(1)	C(1)–C(2)	C(2)–C(3)	C(3)–C(4)	C(4)–C(5)	C(5)–C(6)	C(6)–C(1)
5a	1.473(2)	1.514(2)	1.532(2)	1.538(2)	1.533(2)	1.529(2)	1.516(2)
5b	1.476(2)	1.512(2)	1.530(2)	1.534(2)	1.530(2)	1.527(2)	1.517(2)
5c	1.497(2)	1.496(2)	1.522(2)	1.532(2)	1.535(2)	1.529(2)	1.507(2)
5d	1.492(2)	1.514(2)	1.531(2)	1.537(2)	1.536(2)	1.528(2)	1.517(2)
5e	1.460(2)	1.516(2)	1.529(2)	1.533(2)	1.534(2)	1.530(2)	1.520(2)
5f	1.466(2)	1.513(3)	1.523(3)	1.536(3)	1.529(3)	1.530(3)	1.520(3)
5g	1.471(2)	1.516(2)	1.525(2)	1.535(2)	1.533(2)	1.524(2)	1.515(2)
5h	1.479(2)	1.514(3)	1.525(3)	1.532(3)	1.537(3)	1.524(3)	1.515(3)
5i	1.478(3)	1.510(4)	1.529(4)	1.531(4)	1.529(4)	1.532(4)	1.515(4)
Mean		1.512	1.527	1.534	1.533	1.528	1.516

Table 4 Selected bond distances (Å) for the equatorial derivatives **6a–6g**

Compound	C(1)–O(1)	C(1)–C(2)	C(2)–C(3)	C(3)–C(4)	C(4)–C(5)	C(5)–C(6)	C(6)–C(1)
6a	1.463(2)	1.514(2)	1.529(2)	1.537(2)	1.536(2)	1.535(2)	1.514(2)
Molecule 1							
6a	1.468(2)	1.512(2)	1.526(2)	1.541(2)	1.539(2)	1.537(2)	1.514(2)
Molecule 2							
6b	1.473(2)	1.514(2)	1.531(2)	1.533(2)	1.536(2)	1.529(2)	1.511(2)
6c	1.491(2)	1.504(2)	1.533(2)	1.539(2)	1.525(2)	1.531(2)	1.503(2)
6d	1.487(2)	1.510(2)	1.534(2)	1.527(2)	1.537(2)	1.528(2)	1.511(2)
6e	1.471(2)	1.503(2)	1.530(2)	1.537(2)	1.522(2)	1.534(2)	1.516(2)
6f	1.488(2)	1.506(2)	1.525(2)	1.531(2)	1.533(2)	1.528(2)	1.504(2)
6g	1.487(2)	1.510(2)	1.532(2)	1.534(2)	1.531(2)	1.532(2)	1.510(2)
Molecule 1							
6g	1.492(2)	1.510(2)	1.529(2)	1.536(2)	1.533(2)	1.529(2)	1.509(2)
Molecule 2							
Mean		1.509	1.530	1.535	1.532	1.531	1.510

Table 5 Selected bond distances (Å) for the 2-adamantyl derivatives **7a–7f**

Compound	C(2)–O(1)	C(1)–C(7)	C(3)–C(9)	C(1)–C(6)	C(3)–C(4)	C(1)–C(2)	C(2)–C(3)	C(7)–C(8)	C(8)–C(9)	C(8)–C(10)
7a	1.456(1)	1.533(2)	1.539(2)	1.534(2)	1.534(2)	1.526(2)	1.534(2)	1.534(2)	1.532(2)	1.535(2)
7b	1.478(2)	1.552(2)	1.554(2)	1.538(2)	1.543(2)	1.518(2)	1.488(2)	1.499(2)	1.529(2)	1.539(2)
7c	1.481(2)	1.545(3)	1.537(3)	1.530(3)	1.528(3)	1.513(3)	1.520(3)	1.531(3)	1.538(3)	1.531(3)
Molecule 1										
7c	1.481(3)	1.535(3)	1.540(3)	1.530(4)	1.508(4)	1.523(4)	1.504(3)	1.540(4)	1.528(3)	1.518(3)
Molecule 2										
7d	1.487(2)	1.534(2)	1.537(3)	1.525(3)	1.530(3)	1.522(2)	1.527(2)	1.534(2)	1.536(3)	1.531(3)
7e	1.492(1)	1.540(2)	1.537(2)	1.536(2)	1.533(2)	1.521(2)	1.522(2)	1.535(2)	1.536(2)	1.533(2)
7f	1.485(2)	1.536(2)	1.538(2)	1.534(2)	1.533(2)	1.516(2)	1.526(2)	1.535(2)	1.533(2)	1.537(2)

ring systems of the two molecules of **7c** is approximately 3.7 Å. This brings the nitro groups of the two molecules into close contact with each other; the O(4) ⋯ N(2') and O(4') ⋯ N(2) distances which are 2.789(2) and 2.851(2) Å, respectively, and are well within the sum of the van der Waals radii of nitrogen and oxygen which is 3.05 Å.²⁴ We believe that these short nitro–nitro distance represent weak bonding interactions, consistent with this is the observation that N(2') deviates from the plane of its attached substituents (O(5'), O(6') and C(15')) by 0.008 Å towards O(2), while N(2) deviates from the plane defined by O(5), O(6) and C(15) by 0.003 Å towards O(2'), the smaller deviation in the latter case is consistent with the greater distance between the N(2) and O(2'). Similar nitro–nitro interactions have been reported in the crystal structure of the picrates **5c** and **6c**,¹⁵ in the crystal structure of nitromethane²⁵ and in a nitromethane solvate²⁶ although in these examples the N ⋯ O distances are longer and hence the interactions weaker (3.02–3.05 Å). Weaker nitro–nitro interactions also exist between each pair of molecules of **7c** and other pairs of molecules extending up

the b axis, these secondary interactions are characterised by the distances; O(3') ⋯ N(2) of 2.907(2) Å and O(3) ⋯ N(2') of 3.111(2) Å.

Examination of the structural parameters in Tables 3 and 4 show excellent agreement between those C–C bonds which are related by the approximate local plane of symmetry bisecting the C(1)–O(1) and C(4)–C(7) bonds. The C–C bonds of the cyclohexane rings show systematic variations; the mean C(1)–C(2) and C(1)–C(6) bonds distances is 1.512 Å. The C(2)–C(3) and C(5)–C(6) distances are 1.529 Å, and the mean C(3)–C(4) and C(4)–C(5) are 1.534 Å. These bond distance variations can be adequately accounted for by hybridisation effects;²⁷ the electronegative substituent attached to C(1) is expected to increase the s-character of C(1) which would lead to shortening of the C(1)–C(2) and C(1)–C(6) bond distances. In addition the electropositive substituent attached to C(4) may be expected to decrease the s-character at C(4), leading to lengthening of the C(3)–C(4) and C(4)–C(5) bonds. The variation in the C–C bond distances may also have a hyperconjugative component, for

example $\sigma_{\text{C-H}}-\sigma_{\text{C-O}}^*$ interactions in the axial structures and $\sigma_{\text{C-C}}-\sigma_{\text{C-O}}^*$ in the equatorial structures would be expected to result in shortening of the C(1)–C(2) and C(1)–C(6) distances, in addition, lengthening of the C(2)–C(3) and C(5)–C(6) distances in the equatorial structures compared with the axial structures would be expected. However, the C(2)–C(3) and C(5)–C(6) distances, whose mean values are 1.531 Å in the equatorial structures and 1.528 Å in the axial structures are not significantly different from one another, implying that hyperconjugative effects, if present, are small.

A plot of C–OR bond distance vs. $\text{p}K_{\text{a}}(\text{ROH})$ has been constructed for the axial **5**, equatorial **6**, and 2-adamantyl **7** derivatives,† these are presented in Figs. 5, 6 and 7. From these plots the following relationships between the C(1)–O(1) bond distance and $\text{p}K_{\text{a}}$ were established:

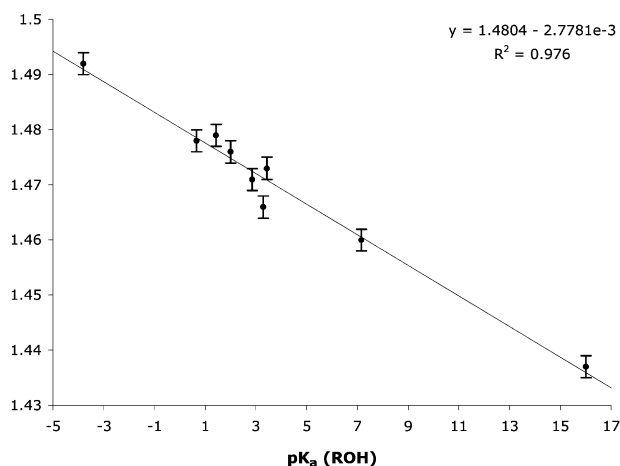


Fig. 5 $r(\text{C-O})$ vs. $\text{p}K_{\text{a}}(\text{ROH})$ relationship for the axial cyclohexyl derivatives **5a–b**, **5d–i** and the unsubstituted axial alcohol. †

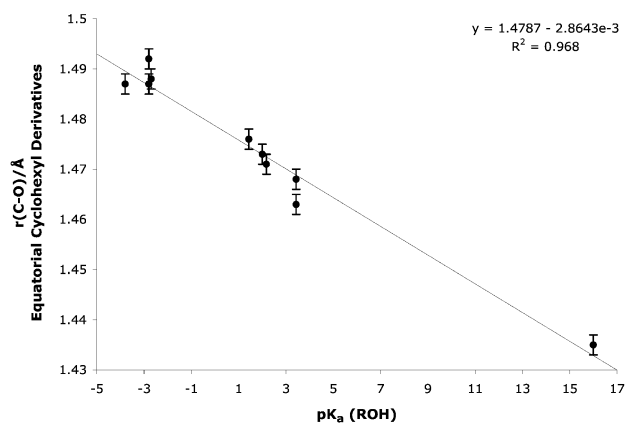


Fig. 6 $r(\text{C-O})$ vs. $\text{p}K_{\text{a}}(\text{ROH})$ relationship for the equatorial cyclohexyl derivatives **6a–b**, **6d–g** and unsubstituted equatorial alcohol and equatorial 2,4-dinitrobenzoate derivatives. †

$$5: r_{\text{C-O}}/\text{Å} = 1.480 - 2.77 \times 10^{-3} \text{p}K_{\text{a}}(\text{ROH}); R^2 = 0.976 \quad (4)$$

$$6: r_{\text{C-O}}/\text{Å} = 1.487 - 2.86 \times 10^{-3} \text{p}K_{\text{a}}(\text{ROH}); R^2 = 0.968 \quad (5)$$

$$7: r_{\text{C-O}}/\text{Å} = 1.482 - 3.05 \times 10^{-3} \text{p}K_{\text{a}}(\text{ROH}); R^2 = 0.958 \quad (6)$$

Eqns. (4)–(6) demonstrate a clear relationship between the C–OR bond distance and the electron demand of the OR

† These plots also include data from previously determined low-temperature structures of appropriate derivatives; a C–OH bond distance for the axial alcohol has been estimated from several low-temperature structures of appropriate derivatives found in the Cambridge Crystallographic Database,²⁹ the low-temperature structure of 2-adamantanol has been previously reported,³⁰ and the equatorial alcohol and 2,4-dinitrobenzoate have also been reported.¹⁸

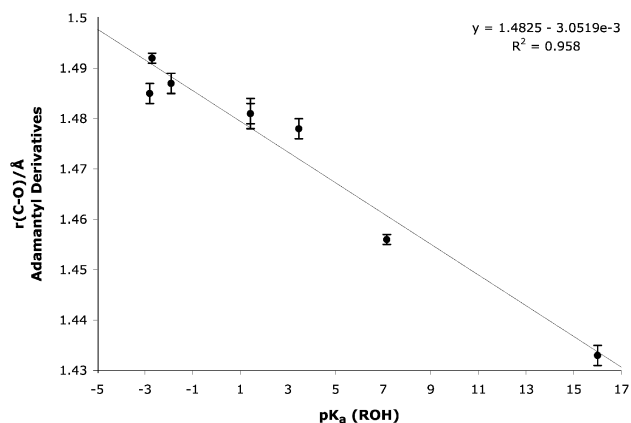


Fig. 7 $r(\text{C-O})$ vs. $\text{p}K_{\text{a}}(\text{ROH})$ relationship for the 2-adamantyl derivatives **7a–7f** and 2-adamantanol. †

substituent, however the correlation coefficients in all cases is modest. The slope of eqn. (4) (-2.77×10^{-3}) represents a measure of the donor ability of the two axial C–H bonds at C(2) and C(6) of *cis* derivatives **5** while the slope of eqn. (5) (-2.86×10^{-3}) reflects the donor ability of the antiperiplanar C–C bonds (C(2)–C(3) and C(5)–C(6)) in the *trans* derivatives **6**. The slope of eqn. (6) (-3.05×10^{-3}) represents the combined donor abilities of the bonds C(1)–C(7) and C(3)–C(9) in the adamantyl derivatives **7**. Given the modest correlation coefficients, and given that the differences in the slope of these three equations is small no conclusions can be made about the relative donor abilities of C–H bonds and C–C bonds. The failure of the *variable oxygen probe* to distinguish the σ -donor abilities of C–H and C–C bonds in these systems is very likely due to these bonds being relatively weak σ -donors and therefore the response of the C–OR bond distance to the $\text{p}K_{\text{a}}(\text{ROH})$ is relatively weak and is likely masked by statistical variations and packing effects.²⁸

Experimental

General

Anhydrous tetrahydrofuran and diethyl ether were distilled from sodium benzophenone ketyl and sodium metal under a nitrogen atmosphere. Anhydrous pyridine was distilled from calcium hydride and stored over 4Å molecular sieves. Petroleum ether (petrol) refers to the fraction boiling at 40–60°C. Benzoyl chlorides were prepared by stirring the benzoic acid derivative and oxalyl chloride (2 equiv.) in CH_2Cl_2 with a catalytic amount of DMF at rt overnight. The crude benzoyl chloride derivative then underwent appropriate purification. 2-Adamantanol was purchased from the Aldrich Chemical Company and all other commercial reagents were used as received. Where necessary, all air- and moisture-sensitive reactions were performed in flame-dried glassware under a nitrogen atmosphere, which was purified by passage over activated 4Å molecular sieves and BASF R3–11 copper catalyst. All melting points were determined on single crystals using a Reichert–Jung hot stage melting point apparatus and are uncorrected. All proton nuclear magnetic resonance (^1H NMR) and proton decoupled carbon nuclear magnetic resonance (^{13}C NMR) spectra were recorded in deuteriochloroform solutions at ambient temperature with residual chloroform as the internal reference.

Synthesis

***cis*-4-*tert*-Butylcyclohexanol 5.** To a stirring solution of L-selectride (48.7 mL, 0.048 mol) in dry THF (50 mL) at -78°C was added dropwise a solution of 4-*tert*-butylcyclohexanone (5.01 g, 0.032 mol) in dry THF (25 mL). The temperature was maintained for 2 h before the reaction mixture was allowed to

stirred overnight at rt. The mixture was cooled to 0°C before careful quenching with water. This was followed by warming to rt before the addition of sodium hydroxide (20 mL, 3 M) followed by hydrogen peroxide (20 mL, 30%) and stirring for 2 h. The mixture was extracted with Et₂O (3×), and the combined organic fractions were washed with saturated aqueous NaCl and water, dried (MgSO₄), filtered, and concentrated *in vacuo* to yield **5** as a white solid (5 g, 98%), mp 80–82.5°C (lit.³¹ 82–83°C); δ_H (300 MHz, CDCl₃) 0.85 (9H, s), 1.30–1.85 (9H, m), 4.03 (1H, br t, *J* 2.5); δ_C (300 MHz, CDCl₃) 20.86, 27.45, 32.53, 33.34, 47.98, 65.89.

trans-4-tert-Butylcyclohexanol 6. To a suspension of lithium aluminium hydride (1.84 g, 0.049 mol) in dry Et₂O (40 mL) at 0°C was added dropwise a solution of 4-*tert*-butylcyclohexanone (5.125 g, 0.033 mol) in dry Et₂O (25 mL). The reaction mixture was then allowed to stir at 0°C for 2 h and then quenched with water. The suspension was filtered through Celite and the filtrate was extracted with Et₂O (3×), and the combined organic fractions were washed with water, dried (MgSO₄), filtered, and concentrated *in vacuo* to yield **6** as a white solid which was 95% pure (3.95 g, 75%); mp 67–68.5°C (lit.³¹ 81–82°C, 100% pure); δ_H (300 MHz, CDCl₃) 0.78 (9H, s), 0.92–1.96 (9H, m), 3.43 (1H, sept, *J* 4.5 Hz); δ_C (300 MHz, CDCl₃) 25.53, 27.55, 32.16, 35.89, 47.10, 70.95.

cis-4-tert-Butylcyclohexyl 4-nitrophenoxide 5e. A suspension of NaH (0.3 g, 60%) in dry THF (10 mL) was treated with a solution of alcohol **5** (500 mg, 3.2 mmol) in dry THF (10 mL). The resulting solution was stirred at rt for 1 h then cooled to –78°C before a solution of 1-fluoro-4-nitrobenzene (0.68 g, 0.51 mL, 4.8 mmol) in dry THF (10 mL) was added. The mixture immediately produced a bright yellow precipitate. The reaction was stirred at rt for 24 h. Excess NaH was destroyed by the addition of water, and the resulting mixture was extracted with Et₂O (3×). The combined organic fractions were washed with water, dried (MgSO₄), filtered, and concentrated *in vacuo* to yield **5e** as a yellow solid (880 mg, 97%), which was recrystallised from MeOH to give pale yellow needles: mp 80–83°C; δ_H (300 MHz, CDCl₃) 0.87 (9H, s), 1.08–2.14 (9H, m), 4.66 (1H, br s), 6.95 (2H, d, *J* 9.3 Hz), 8.18 (2H, d, *J* 9.3 Hz); δ_C (300 MHz, CDCl₃) 20.22, 27.37, 30.02, 32.48, 47.43, 72.44, 115.37, 125.86, 140.82, 163.11.

2-Adamantyl 4-nitrophenoxide 7a. A suspension of NaH (0.1 g 60%) in dry THF (10 mL) was treated with a solution of 2-adamantanol (200 mg, 1.32 mmol) in dry THF (10 mL). The resulting solution was stirred at rt for 1 h then cooled to –78°C before a solution of 1-fluoro-4-nitrobenzene (0.29 g, 0.21 mL, 0.2 mmol) in dry THF (5 mL) was added. The reaction was stirred for 72 h at rt. Excess NaH was destroyed by the addition of water, and the resulting mixture was extracted with Et₂O (3×). The combined organic fractions were washed with water, dried (MgSO₄), filtered, and concentrated *in vacuo* to yield **7a** as a yellow solid (326.5 mg, 90%), which was recrystallised from MeOH to give golden sheets: mp 84.5–85.5°C; δ_H (300 MHz, CDCl₃) 1.5–2.2 (14H, m), 4.50 (1H, br s), 6.91 (2H, d, *J* 9.3 Hz), 8.12 (2H, d, *J* 9.3 Hz); δ_C (300 MHz, CDCl₃) 26.84, 26.94, 31.16, 31.21, 36.03, 37.06, 80.27, 115.24, 125.71, 140.70, 162.92.

General procedure for the esterification of alcohols with benzoyl, sulfonyl or acetyl chlorides. The alcohol (50 mg) was stirred in pyridine (5 mL) for 30 min and then treated with either benzoyl, sulfonyl or acetate chloride (1.5 equiv.), which was added all at once. The reaction was stirred at rt for 4 h or until precipitation of pyridine hydrochloride was complete. Water was then added and undissolved solids were filtered off. The filtrate was then extracted with Et₂O (3×), and the combined organic fractions were washed with saturated aqueous CuSO₄, water, saturated aqueous NaHCO₃ and water then

dried (MgSO₄), filtered, and concentrated *in vacuo* to the crude product which was subsequently recrystallised to produce crystals of X-ray quality.

cis-4-tert-Butylcyclohexyl 4-chloro-3-nitrobenzoate 5f. mp 139–141°C (colourless plates from MeOH); δ_H (300 MHz, CDCl₃) 0.88 (9H, s), 1.10–2.11 (9H, m), 5.28 (1H, br s), 7.64 (1H, d, *J* 8.4 Hz), 8.14 (1H, dd, *J* 1.8 and 8.4 Hz), 8.48 (1H, d, *J* 1.8 Hz); δ_C (300 MHz, CDCl₃) 21.75, 27.35, 30.47, 32.50, 47.25, 71.74, 126.44, 131.05, 131.23, 132.11, 133.36, 147.89, 162.97.

cis-4-tert-Butylcyclohexyl 3,5-dinitrobenzoate 5g. mp 118–119.5°C (pale yellow needles from MeOH); δ_H (300 MHz, CDCl₃) 0.91 (9H, s), 1.15–2.16 (9H, m), 5.37 (1H, br t, *J* 2.5), 9.14 (2H, m), 9.22 (1H, m); δ_C (300 MHz, CDCl₃) 21.74, 27.32, 30.43, 32.53, 47.16, 72.90, 122.11, 129.24, 134.80, 148.65, 161.74.

cis-4-tert-Butylcyclohexyl 2,4-dinitrobenzoate 5h. mp 89.5–90.5°C (pale yellow needles from Et₂O); δ_H (300 MHz, CDCl₃) 0.84 (9H, s), 1.04–2.10 (9H, m), 5.34 (1H, br s), 7.99 (1H, d, *J* 8.4 Hz), 8.52 (1H, dd, *J* 1.5 and 8.1 Hz), 8.71 (1H, d, *J* 1.5 Hz); δ_C (300 MHz, CDCl₃) 21.65, 27.35, 30.31, 32.48, 47.29, 73.82, 119.34, 127.09, 131.58, 133.04, 148.87, 162.93.

cis-4-tert-Butylcyclohexyl trichloroacetate 5i. mp 55–57°C (pale brown needles from MeOH); δ_H (300 MHz, CDCl₃) 0.85 (9H, s), 1.03–2.11 (9H, m), 5.14 (1H, br t, *J* 2.4); δ_C (300 MHz, CDCl₃) 21.30, 27.32, 30.00, 32.50, 47.08, 76.04, 90.50, 161.16.

trans-4-tert-Butylcyclohexyl 2-nitrobenzoate 6e. mp 88–90°C (pale yellow needles from petrol); δ_H (300 MHz, CDCl₃) 0.83 (9H, s), 0.99–2.16 (9H, m), 4.87 (1H, sept, *J* 4.5 Hz), 7.87–7.55 (4H, m); δ_C (300 MHz, CDCl₃) 25.28, 27.48, 31.45, 32.19, 47.86, 76.14, 123.66, 138.11, 129.76, 133.40, 132.70, 148.13, 164.84.

trans-4-tert-Butylcyclohexyl 4-toluenesulfonate 6f. mp 75.5–77°C (colourless needles from petrol); δ_H (300 MHz, CDCl₃) 0.78 (9H, s), 0.93–1.96 (9H, m), 2.42 (3H, s), 4.32 (1H, sept, *J* 4.5 Hz), 7.31 (2H, d, *J* 8.1 Hz), 7.77 (2H, d, *J* 8.4 Hz); δ_C (300 MHz, CDCl₃) 25.42, 27.41, 32.10, 32.77, 46.43, 82.55, 127.49, 129.64, 134.66, 141.25.

trans-4-tert-Butylcyclohexyl benzenesulfonate 6g. mp 33–35°C (pale yellow needles from petrol); δ_H (300 MHz, CDCl₃) 0.79 (9H, s), 1.86–1.98 (9H, m), 4.37 (1H, sept, *J* 4.5 Hz), 7.52 (2H, m), 7.61 (1H, m), 7.90 (2H, m); δ_C (300 MHz, CDCl₃) 25.45, 27.43, 32.13, 32.81, 46.44, 82.90, 127.47, 129.05, 133.35, 137.60.

2-Adamantyl 3-nitrobenzoate 7b. mp 68–70°C (colourless needles from MeOH); δ_H (300 MHz, CDCl₃) 1.55–2.20 (14H, m), 5.24 (1H, br s), 7.66 (1H, t, *J* 7.95 Hz), 8.41 (2H, d, *J* 7.8 Hz), 8.88 (1H, s); δ_C (300 MHz, CDCl₃) 26.80, 27.08, 31.84, 31.87, 36.17, 37.13, 78.68, 124.31, 127.05, 129.47, 132.71, 135.10, 148.14, 163.55.

2-Adamantyl 2,4-dinitrobenzoate 7c. mp 134–135.5°C (pale yellow blocks from Et₂O); δ_H (400 MHz, CDCl₃) 1.56–2.11 (14H, m), 5.22 (1H, br s), 7.97 (1H, dd, *J* 2 and 8.4 Hz), 8.50 (1H, dt, *J* 2 and 8.4 Hz), 8.70 (1H, t, *J* 2 Hz); δ_C (400 MHz, CDCl₃) 26.72, 26.87, 31.55, 31.58, 36.17, 37.02, 80.91, 119.30, 127.19, 131.36, 133.08, 148.13, 148.70, 162.87.

2-Adamantyl methanesulfonate 7d. mp 51–53°C (pale yellow plates from Et₂O); δ_H (300 MHz, CDCl₃) 1.55–2.15 (14H, m), 2.99 (3H, s), 4.84 (1H, br s); δ_C (300 MHz, CDCl₃) 26.42, 26.73, 31.04, 32.90, 36.25, 36.93, 38.65, 85.93.

2-Adamantyl 4-toluenesulfonate 7e. mp 68–70°C (pale yellow plates from MeOH); δ_{H} (300 MHz, CDCl_3) 1.46–2.14 (14H, m), 2.43 (3H, s), 4.68 (1H, br s), 7.32 (2H, d, J 7.5 Hz), 7.79 (2H, d, J 6.9 Hz); δ_{C} (300 MHz, CDCl_3) 21.29, 26.26, 26.52, 30.80, 32.37, 36.06, 36.76, 85.97, 127.14, 129.45, 134.58, 144.03.

2-Adamantyl benzenesulfonate 7f. mp 79–82°C (pale yellow blocks from MeOH); δ_{H} (300 MHz, CDCl_3) 1.46–2.12 (14H, m), 2.43 (3H, s), 4.72 (1H, br t, J 2.4), 7.53 (2H, m), 7.63 (1H, m), 7.92 (2H, m); δ_{C} (300 MHz, CDCl_3) 26.32, 26.59, 30.89, 32.49, 36.16, 36.84, 86.46, 127.22, 128.93, 133.22, 137.66.

Crystallography

Data for structures **5e**, **5g–5i**, **6f**, **7a–7b**, **7d** and **7f** were collected on an Enraf-Nonius CAD-4 Diffractometer using Mo- $K\alpha$ radiation ($\lambda = 0.71069 \text{ \AA}$, graphite monochromator) or Ni-filtered Cu- $K\alpha$ radiation ($\lambda = 1.5418 \text{ \AA}$) at 130.0(1) K, data for structures **5f**, **6e**, **6g**, **7c** and **7e** were collected on a Nonius Kappa CCD Area-Detector Diffractometer at 130.0(1) K. The crystals were mounted on a glass fibre usually using low-temperature silicone oil and was then flash frozen by placing directly on a goniometer head under a stream of nitrogen gas at 130 K. The temperature was controlled using an Oxford Cryostream cooling device. The data were corrected for Lorentz and polarization effects³² for absorption where appropriate (ABSORB)³³ and extinction³⁴ where appropriate. Structures were solved by direct methods (SHELXS-86)³⁵ and were refined on F^2 (SHELXL-97).³⁴ All non hydrogens were refined anisotropically, while the treatment of hydrogen atoms depended on the data/reflection ratio, in some structures hydrogen atoms were refined isotropically without restraint while in others they were constrained. Thermal ellipsoids plots were generated using the program ORTEP-3³⁶ all programs were implemented within the suite WINGX.³⁷

Crystal data for 5e. $\text{C}_{16}\text{H}_{23}\text{NO}_3$, $M = 277.36$, $T = 130.0(1) \text{ K}$, $\lambda = 0.71069 \text{ \AA}$, triclinic, space group $P\bar{1}$, $a = 6.179(2)$, $b = 11.071(3)$, $c = 11.130(2) \text{ \AA}$, $\alpha = 100.57(2)^\circ$, $\beta = 90.17(2)^\circ$, $\gamma = 95.16(2)^\circ$, $V = 745.3(3) \text{ \AA}^3$, $Z = 2$, $D_c = 1.236 \text{ Mg m}^{-3}$, $\mu(\text{Mo-K}\alpha) = 0.085 \text{ mm}^{-1}$, $F(000) = 300$, crystal size $0.50 \times 0.40 \times 0.12 \text{ mm}$. 2888 reflections measured, 2622 independent reflections ($R_{\text{int}} = 0.0196$) and the final $wR(F^2)$ was 0.1252 and final R was 0.0439 for 2196 unique data with $[I > 2\sigma(I)]$.

Crystal data for 5f. $\text{C}_{17}\text{H}_{22}\text{ClNO}_4$, $M = 339.81$, $T = 130.0(1) \text{ K}$, $\lambda = 0.71069 \text{ \AA}$, monoclinic, space group $P2_1/n$, $a = 6.975(3)$, $b = 36.618(8)$, $c = 7.034(2) \text{ \AA}$, $\beta = 107.555(1)^\circ$, $V = 1713.1(1) \text{ \AA}^3$, $Z = 4$, $D_c = 1.318 \text{ Mg m}^{-3}$, $\mu(\text{Mo-K}\alpha) = 0.242 \text{ mm}^{-1}$, $F(000) = 720$, crystal size $0.20 \times 0.20 \times 0.10 \text{ mm}$. 10738 reflections measured, 2860 independent reflections ($R_{\text{int}} = 0.0546$) and the final $wR(F^2)$ was 0.1252 and final R was 0.0417 for 1991 unique data with $[I > 2\sigma(I)]$.

Crystal data for 5g. $\text{C}_{17}\text{H}_{22}\text{N}_2\text{O}_6$, $M = 350.37$, $T = 130.0(1) \text{ K}$, $\lambda = 1.5418 \text{ \AA}$, monoclinic, space group $P2_1/c$, $a = 16.441(2)$, $b = 5.981(1)$, $c = 18.722(2) \text{ \AA}$, $\beta = 109.47(2)^\circ$, $V = 1735.7(6) \text{ \AA}^3$, $Z = 4$, $D_c = 1.341 \text{ Mg m}^{-3}$, $\mu(\text{Cu-K}\alpha) = 0.856 \text{ mm}^{-1}$, $F(000) = 744$, max. min. transmission 0.95, 0.69, crystal size $0.75 \times 0.25 \times 0.06 \text{ mm}$. 3027 reflections measured, 2923 independent reflections ($R_{\text{int}} = 0.0172$) and the final $wR(F^2)$ was 0.1014 and final R was 0.0360 for 2622 unique data with $[I > 2\sigma(I)]$.

Crystal data for 5h. $\text{C}_{17}\text{H}_{22}\text{N}_2\text{O}_6$, $M = 350.37$, $T = 130.0(1) \text{ K}$, $\lambda = 0.71069 \text{ \AA}$, monoclinic, space group $P2_1/c$, $a = 15.388(5)$, $b = 7.129(1)$, $c = 16.839(6) \text{ \AA}$, $\beta = 112.56(3)^\circ$, $V = 1705.9(9) \text{ \AA}^3$, $Z = 4$, $D_c = 1.364 \text{ Mg m}^{-3}$, $\mu(\text{Mo-K}\alpha) = 0.104 \text{ mm}^{-1}$, $F(000) = 744$, crystal size $0.60 \times 0.37 \times 0.12 \text{ mm}$. 3114 reflections measured, 2993 independent reflections ($R_{\text{int}} = 0.0203$) and the final $wR(F^2)$ was 0.1032 and final R was 0.0421 for 2323 unique data with $[I > 2\sigma(I)]$.

Crystal data for 5i. $\text{C}_{12}\text{H}_{19}\text{Cl}_3\text{O}_2$, $M = 301.62$, $T = 130.0(1) \text{ K}$, $\lambda = 1.5418 \text{ \AA}$, monoclinic, space group $P2_1$, $a = 9.654(1)$, $b = 6.026(1)$, $c = 13.044(2) \text{ \AA}$, $\beta = 107.09(1)^\circ$, $V = 725.3(3) \text{ \AA}^3$, $Z = 2$, $D_c = 1.381 \text{ Mg m}^{-3}$, $\mu(\text{Cu-K}\alpha) = 5.630 \text{ mm}^{-1}$, $F(000) = 316$, max. min. transmission 0.67, 0.22, crystal size $0.60 \times 0.17 \times 0.08 \text{ mm}$. 1733 reflections measured, 1636 independent reflections ($R_{\text{int}} = 0.0224$) and the final $wR(F^2)$ was 0.0966 and final R was 0.0371 for 1589 unique data with $[I > 2\sigma(I)]$.

Crystal data for 6e. $\text{C}_{17}\text{H}_{23}\text{NO}_4$, $M = 305.36$, $T = 130.0(1) \text{ K}$, $\lambda = 0.71069 \text{ \AA}$, monoclinic, space group $P2_1/n$, $a = 6.237(1)$, $b = 12.773(2)$, $c = 20.439(4) \text{ \AA}$, $\beta = 97.722(1)^\circ$, $V = 1613.49(5) \text{ \AA}^3$, $Z = 4$, $D_c = 1.257 \text{ Mg m}^{-3}$, $\mu(\text{Mo-K}\alpha) = 0.089 \text{ mm}^{-1}$, $F(000) = 654$, crystal size $0.25 \times 0.07 \times 0.07 \text{ mm}$. 16946 reflections measured, 3719 independent reflections ($R_{\text{int}} = 0.0367$) and the final $wR(F^2)$ was 0.0943 and final R was 0.0463 for 2826 unique data with $[I > 2\sigma(I)]$.

Crystal data for 6f. $\text{C}_{17}\text{H}_{26}\text{SO}_3$, $M = 310.44$, $T = 130.0(1) \text{ K}$, $\lambda = 1.5418 \text{ \AA}$, triclinic, space group $P\bar{1}$, $a = 6.2680(1)$, $b = 10.409(1)$, $c = 13.190(2) \text{ \AA}$, $\alpha = 94.300(1)^\circ$, $\beta = 95.040(1)^\circ$, $\gamma = 98.830(1)^\circ$, $V = 843.6(3) \text{ \AA}^3$, $Z = 2$, $D_c = 1.222 \text{ Mg m}^{-3}$, $\mu(\text{Cu-K}\alpha) = 1.761 \text{ mm}^{-1}$, $F(000) = 336$, crystal size $0.35 \times 0.15 \times 0.10 \text{ mm}$. 3519 reflections measured, 3204 independent reflections ($R_{\text{int}} = 0.0158$) and the final $wR(F^2)$ was 0.0954 and final R was 0.0375 for 2819 unique data with $[I > 2\sigma(I)]$.

Crystal data for 6g. $\text{C}_{16}\text{H}_{24}\text{SO}_3$, $M = 296.41$, $T = 130.0(1) \text{ K}$, $\lambda = 0.71069 \text{ \AA}$, monoclinic, space group $P2_1/c$, $a = 24.736(3)$, $b = 6.202(1)$, $c = 20.939(4) \text{ \AA}$, $\beta = 100.487(1)^\circ$, $V = 3158.68(9) \text{ \AA}^3$, $Z = 8$, $D_c = 1.247 \text{ Mg m}^{-3}$, $\mu(\text{Mo-K}\alpha) = 0.210 \text{ mm}^{-1}$, $F(000) = 1280$, crystal size $0.40 \times 0.10 \times 0.05 \text{ mm}$. 38021 reflections measured, 7783 independent reflections ($R_{\text{int}} = 0.0579$) and the final $wR(F^2)$ was 0.0989 and final R was 0.0443 for 5301 unique data with $[I > 2\sigma(I)]$.

Crystal data for 7a. $\text{C}_{16}\text{H}_{19}\text{NO}_3$, $M = 273.32$, $T = 130.0(1) \text{ K}$, $\lambda = 1.5418 \text{ \AA}$, triclinic, space group $P\bar{1}$, $a = 6.767(2)$, $b = 9.556(3)$, $c = 10.887(3) \text{ \AA}$, $\alpha = 99.43(3)^\circ$, $\beta = 90.68(2)^\circ$, $\gamma = 105.38(2)^\circ$, $V = 668.5(3) \text{ \AA}^3$, $Z = 2$, $D_c = 1.358 \text{ Mg m}^{-3}$, $\mu(\text{Cu-K}\alpha) = 0.759 \text{ mm}^{-1}$, $F(000) = 292$, max. min. transmission 0.84, 0.73, crystal size $0.50 \times 0.38 \times 0.26 \text{ mm}$. 2833 reflections measured, 2689 independent reflections ($R_{\text{int}} = 0.0095$) and the final $wR(F^2)$ was 0.0896 and final R was 0.0355 for 2645 unique data with $[I > 2\sigma(I)]$.

Crystal data for 7b. $\text{C}_{17}\text{H}_{19}\text{NO}_4$, $M = 301.33$, $T = 130.0(1) \text{ K}$, $\lambda = 1.5418 \text{ \AA}$, triclinic, space group $P\bar{1}$, $a = 7.539(3)$, $b = 8.479(2)$, $c = 12.043(3) \text{ \AA}$, $\alpha = 75.30(2)^\circ$, $\beta = 76.86(2)^\circ$, $\gamma = 88.83(3)^\circ$, $V = 724.6(4) \text{ \AA}^3$, $Z = 2$, $D_c = 1.381 \text{ Mg m}^{-3}$, $\mu(\text{Cu-K}\alpha) = 0.809 \text{ mm}^{-1}$, $F(000) = 320$, crystal size $0.50 \times 0.40 \times 0.07 \text{ mm}$. 4014 reflections measured, 2761 independent reflections ($R_{\text{int}} = 0.0183$) and the final $wR(F^2)$ was 0.1096 and final R was 0.0402 for 2635 unique data with $[I > 2\sigma(I)]$.

Crystal data for 7c. $\text{C}_{17}\text{H}_{18}\text{N}_2\text{O}_6$, $M = 346.33$, $T = 130.0(1) \text{ K}$, $\lambda = 0.71069 \text{ \AA}$, monoclinic, space group $P2_1/c$, $a = 29.189(6)$, $b = 7.0518(1)$, $c = 15.415(3) \text{ \AA}$, $\beta = 93.717(1)^\circ$, $V = 3166.3(1) \text{ \AA}^3$, $Z = 8$, $D_c = 1.453 \text{ Mg m}^{-3}$, $\mu(\text{Mo-K}\alpha) = 0.111 \text{ mm}^{-1}$, $F(000) = 1456$, crystal size $0.16 \times 0.12 \times 0.07 \text{ mm}$. 19999 reflections measured, 5513 independent reflections ($R_{\text{int}} = 0.0638$) and the final $wR(F^2)$ was 0.1377 and final R was 0.0481 for 3597 unique data with $[I > 2\sigma(I)]$.

Crystal data for 7d. $\text{C}_{11}\text{H}_{18}\text{SO}_3$, $M = 230.31$, $T = 130.0(1) \text{ K}$, $\lambda = 0.71069 \text{ \AA}$, orthorhombic, space group $Pbca$, $a = 9.000(2)$, $b = 9.594(4)$, $c = 26.225(7) \text{ \AA}$, $V = 2264(1) \text{ \AA}^3$, $Z = 8$, $D_c = 1.351 \text{ Mg m}^{-3}$, $\mu(\text{Mo-K}\alpha) = 0.271 \text{ mm}^{-1}$, $F(000) = 992$, crystal size $0.30 \times 0.30 \times 0.05 \text{ mm}$. 3002 reflections measured, 2585 independent reflections ($R_{\text{int}} = 0.0331$) and the final $wR(F^2)$

was 0.0918 and final R was 0.0375 for 2045 unique data with $[I > 2\sigma(I)]$.

Crystal data for 7e. $C_{17}H_{22}SO_3$, $M = 306.41$, $T = 130.0(1)$ K, $\lambda = 0.71069$ Å, monoclinic, space group $P2_1/c$, $a = 10.124(1)$, $b = 12.551(2)$, $c = 12.409(1)$ Å, $\beta = 106.860(1)^\circ$, $V = 1509.13(3)$ Å³, $Z = 4$, $D_c = 1.349$ Mg m⁻³, $\mu(\text{Mo-K}\alpha) = 0.222$ mm⁻¹, $F(000) = 656$, crystal size $0.15 \times 0.11 \times 0.09$ mm. 24439 reflections measured, 3720 independent reflections ($R_{\text{int}} = 0.0405$) and the final $wR(F^2)$ was 0.1143 and final R was 0.0377 for 3276 unique data with $[I > 2\sigma(I)]$.

Crystal data for 7f. $C_{16}H_{20}SO_3$, $M = 292.38$, $T = 130.0(1)$ K, $\lambda = 1.5418$ Å, monoclinic, space group $P2_1/c$, $a = 11.735(9)$, $b = 11.125(10)$, $c = 11.132(10)$ Å, $\beta = 104.382(7)^\circ$, $V = 1407.8(1)$ Å³, $Z = 4$, $D_c = 1.379$ Mg m⁻³, $\mu(\text{Cu-K}\alpha) = 2.084$ mm⁻¹, $F(000) = 624$, max. min. transmission 0.83, 0.57, crystal size $0.36 \times 0.28 \times 0.10$ mm. 3055 reflections measured, 2900 independent reflections ($R_{\text{int}} = 0.0142$) and the final $wR(F^2)$ was 0.0781 and final R was 0.0308 for 2612 unique data with $[I > 2\sigma(I)]$.

CCDC reference numbers 205439–205452.

See <http://www.rsc.org/suppdata/ob/b3/b303453d/> for crystallographic data in CIF or other electronic format.

Acknowledgements

We thank Dr Alan R. Happer (Canterbury University, New Zealand) for helpful discussions and Dr Gary D. Fallon (Monash University, Australia) for data collection of structures **5f**, **6e**, **6g**, **7c** and **7e**. The Australian Research Council is gratefully acknowledged for its financial support.

References

- 1 J. W. Baker and W. S. Nathan, *J. Am. Chem. Soc.*, 1935, **1844**.
- 2 R. W. J. Taft and I. C. Lewis, *Tetrahedron*, 1959, **5**, 210.
- 3 E. Glyde and R. Taylor, *J. Chem. Soc., Perkin Trans. 2*, 1977, **5**, 678.
- 4 R. Taylor, G. G. Smith and W. H. Wetzel, *J. Am. Chem. Soc.*, 1962, **84**, 4817.
- 5 B. T. Cooney and D. A. R. Happer, *Aust. J. Chem.*, 1987, **40**, 1537.
- 6 P. R. Rablen, R. W. Hoffmann, D. A. Hrovat and W. T. Borden, *J. Chem. Soc., Perkin Trans. 2*, 1999, **8**, 1719.
- 7 A. S. Cieplak, *J. Am. Chem. Soc.*, 1981, **103**, 4540.
- 8 A. J. Briggs, R. Glenn, P. G. Jones, A. J. Kirby and P. Ramaswamy, *J. Am. Chem. Soc.*, 1984, **106**, 6200.
- 9 R. D. Amos, N. C. Handy, P. G. Jones, A. J. Kirby, J. K. Parker, J. M. Percy and M. D. Su, *J. Chem. Soc., Perkin Trans. 2*, 1992, **4**, 549.
- 10 J. M. White and G. B. Robertson, *J. Org. Chem.*, 1992, **57**, 4638.
- 11 V. Y. Chan, C. I. Clark, J. Giordano, A. J. Green, A. Karalis and J. M. White, *J. Org. Chem.*, 1996, **61**, 5227.
- 12 J. M. White and C. I. Clark, in *Stereoelectronic effects of Group IVA metal substituents in organic chemistry*, ed. S. Denmark, New York, 1999.
- 13 J. M. White and G. B. Robertson, *Acta Crystallogr., Sect. C*, 1993, **49**, 347.
- 14 J. M. White, J. Giordano and A. J. Green, *Acta Crystallogr., Sect. C*, 1996, **52**, 2783.
- 15 M. Spiniello and J. M. White, *Acta Crystallogr., Sect. C*, 2002, **58**, o94.
- 16 J. M. White, J. Giordano and A. J. Green, *Acta Crystallogr., Sect. C*, 1996, **52**, 3204.
- 17 *CRC Handbook of Chemistry and Physics*, ed. D. R. Lide, CRC Press, Boca Raton, FL, 2000.
- 18 A. J. Green, J. Giordano and J. M. White, *Aust. J. Chem.*, 2000, **53**, 285.
- 19 J. F. King, in *The Chemistry of Sulfonic Acids, Esters and Derivatives*, ed. S. Patai and Z. Rappoport, Interscience, West Sussex, England, 1991.
- 20 D. C. Wigfield, *Tetrahedron*, 1979, **35**, 449.
- 21 H. C. Brown and S. Krishnamurthy, *J. Am. Chem. Soc.*, 1972, **94**, 7159.
- 22 C. Rafols, M. Roses and E. Bosch, *Anal. Chim. Acta*, 1997, **338**, 127.
- 23 J. A. Dean, *Lange's Handbook of Chemistry*, McGraw-Hill, New York, 1992.
- 24 A. Bondi, *J. Phys. Chem.*, 1964, **68**, 441.
- 25 I. Y. Bagryanskaya and Y. V. Gatilov, *Zh. Strukt. Khim.*, 1983, **24**, 158.
- 26 B. F. Abrahams, P. A. Jackson and R. Robson, *Angew. Chem., Int. Ed.*, 1998, **37**, 2656.
- 27 L. S. Bartell, *Tetrahedron*, 1962, **17**, 177.
- 28 A. Martin and A. G. Orpen, *J. Am. Chem. Soc.*, 1996, **118**, 1464.
- 29 F. H. Allen, S. Bellard, M. D. Brice, B. A. Cartwright, A. Doubleday, H. Higgs, T. Hummelink, B. G. Hummelink-Peters, O. Kennard, W. D. S. Motherwell, J. R. Rogers and D. G. Watson, *Acta Crystallogr., Sect. B*, 1979, **35**, 2331.
- 30 J. A. Kanters, R. W. W. Hooft and A. J. M. Duisenberg, *J. Crystallogr. Spectrosc. Res.*, 1990, **20**, 123.
- 31 S. Winstein and N. J. Holness, *J. Am. Chem. Soc.*, 1955, **77**, 5562.
- 32 R. W. Gable, B. F. Hoskins, A. Linden, I. A. S. McDonald and R. J. Steen, in *Process data, a program for processing of CAD-4 diffractometer data*, The University of Melbourne, Australia, 1994.
- 33 P. Van der Sluis and A. L. Spek, *Acta Crystallogr., Sect. A*, 1990, **46**, 194.
- 34 G. M. Sheldrick, in *SHELXL-97; Program for Crystal Structure Refinement*. University of Göttingen, Germany, 1997.
- 35 G. M. Sheldrick, in *SHELXS-86; Crystallographic Computing 3*, University of Göttingen, Germany, 1986.
- 36 L. J. Farrugia, *J. Appl. Crystallogr.*, 1997, **30**, 565.
- 37 L. J. Farrugia, *J. Appl. Crystallogr.*, 1999, **32**, 837.